

IN SITU SAMPLE PREPARATION AND DETERMINATION OF DAPSONE IN TABLET FORMULATION USING A NEW CHEMICAL MICRO-TOTAL ANALYSIS SYSTEM WITHOUT MICROCHIPS

Ghusoon Jawad Shabaa¹, Rahman Sahib Zabibah²

¹College of Medicine, Jabir Ibn Hayyan Medical University
for Medical and Pharmaceutical Sciences, Najaf, Iraq

²Medical Laboratory Technology Department, College of Medical Technology,
The Islamic University, Najaf, Iraq
Email: ghusoonshabaa@gmail.com

Received 08 July 2023

Accepted 13 October 2023

DOI: 10.59957/jctm.v59.i5.2024.1

ABSTRACT

In this work, a novel study was investigated in situ sample preparation using the green micro total analysis system (μ TAS) without microchips for the determination of dapson. The microchips have been replaced by capillary tubes with very small internal diameters. These capillary tubes are used in the field of human medicine. As a spectrophotometric reagent, 7-chloro-4-nitrobenzoxadiazole (NBD-Cl) was employed. The suggested approach was dependent on the desired medication, NBD-Cl, reacting in an alkali solution to produce a coloured adduct that had $\lambda_{max} = 468$ nm. Investigations have been done into the several physical and chemical factors that affect the measurement, including sample volume, pH, flow rate, the reacting loop, and the volume and amount of NBD-Cl. This method shows the linearity range of 0.5 to 100 $\mu\text{g mL}^{-1}$ with a coefficient of regression R^2 of 0.9989. The regression equation $A = 0.0697C + 0.0034$. Also, the limit of detection was 0.3998 $\mu\text{g mL}^{-1}$. The proposed system has been applied efficaciously to determine the presence of dapson in medical preparations.

Keywords: Micro Total Analysis System (μ TAS), dapson, 7-chloro-4-nitrobenzoxadiazole (NBD-Cl).

INTRODUCTION

Dapson, also known as 4,4-diaminodiphenylsulfone, is an anti-neurotic medicine in addition to its anti-malarial characteristics. Given its medicinal priority, significant research has been conducted to detect and quantified [1, 2]. Numerous analysis methods, such as pulse-polarography [3], flow injection [4], gas chromatography [5, 6], high-performance liquid chromatography [6, 7], cloud point extraction [8], and spectrophotometric methods [9 - 11], have been used to determine the concentration of dapson in plasma, serum, bodily fluids, medicine dosage, and others [12].

Despite first being developed in the early 1990s, μ TAS have had an important effect on several areas and fields during the past two decades [13]. These lab-on-a-chip (LOC) platforms, also known as tiny fluidic mechanisms, may execute laboratory tasks like preparation, preconcentration, separation, and

measurement on one instrument [14]. μ TAS systems have minimal sample usage, a low process cost, and a quick time to analysis due to their compact size and channel diameters of the order of tens of micrometres. Despite these benefits, a significant barrier to microfluidics continues to be determining the presence of analytes in trace quantities [15 - 17]. To overcome this sensitivity barrier, a preconcentration step before detection seems like a suitable alternative [18 - 20]. Microfluidic systems have performed well in several biological investigations in terms of applications, particularly those involving single cells. The use of microfluidic devices is common in various application fields, such as illness assessment, medication screening, and nucleic acid investigation. Additionally, there has been a surge in interest in creating clinical tests for use on microfluidic devices composed of paper in environments with limited resources [21 - 26].

This paper describes in situ preparation sample using a new μ TAS without microchips method for determining

of dapsone in tablet formulation. This work includes the design of new μ TAS in which the microchips have been substituted by using capillary tubes with very small internal diameters. These capillary tubes are used in the field of human medicine (called Embolectomy catheters), specifically in the cardiac catheterization operation, and both the capillaries themselves, as well as the micro-flow cells, have been manufactured to be convenient for the system.

EXPERIMENTAL

Instrumentation

The schematic diagram of the new manufacturing μ TAS without microchips is explained in Fig. 1. It involved from the left to the right of peristaltic pump (Osmatic, Germany), the homemade valve with 4-port using capillary tubes with very small internal diameters Fig. 5, many new designs of valves were developed by researchers [16-18]. UV-Vis spectrophotometer (Apple), manufactured micro flow cell having a capacity equal 25 μ L [13], Kompensograph (C1032) from Siemens, Germany. The tubes from Teflon throughout of i.d. 0.5mm is used.

Chemicals and reagents

In a graduated flask, 0.05 g of dapsone was dissolved in 100 mL of NaOH (0.01 M) to generate a standard solution that contained 500 g mL^{-1} . The NBD-Cl solution was prepared at 0.03 % (w/v) by dissolving a suitable amount in 100 mL of distilled water in a volumetric flask.

Preparation Pharmaceutical Solutions (Tablet solution of Dapsone)

Ten Dapsone tablets were evaluated precisely and ground in a mortar. Using distilled water, a quantity of powder equal to 100 mg of the medicine was dissolved and applied to the sign. The container and what it contained were rather well cracked and filtered. To obtain 1000 $\mu\text{g mL}^{-1}$ of the medicine, the remaining material had been cleaned and diluted with the same solvent [19].

General procedure

As shown in Fig 2 - 5, the first step is to collect those capillary tubes, which are then sorted, cut, and coil according to their internal diameters; those with an internal diameter of 0.01 cm (equivalent to 0.0785 μL for each one cm of tube length) are used as loops to download

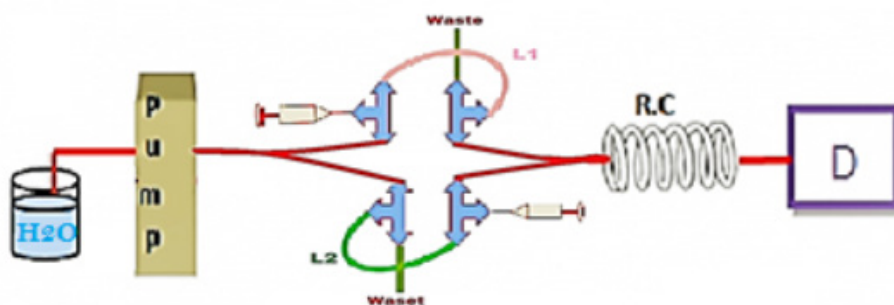


Fig. 1. Manufactured Micro total analysis system (μ TAS).

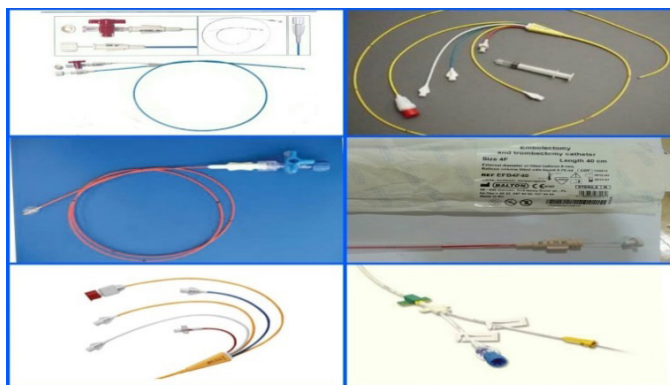


Fig. 2. Some of the used capillary tubes.

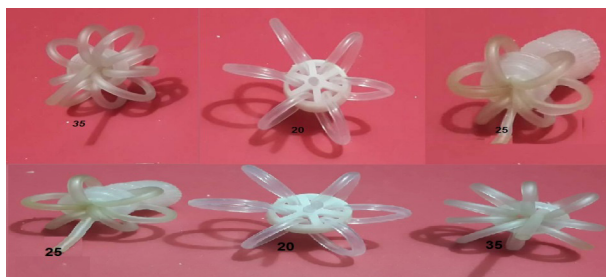


Fig. 3. Some of the capillary tubes used as loops have different lengths.

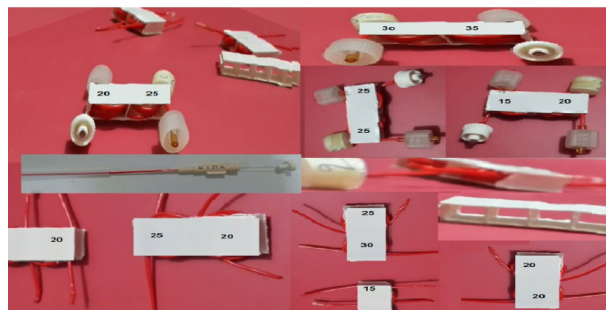


Fig. 4. Some of the capillary tubes used as reaction coils have different lengths.

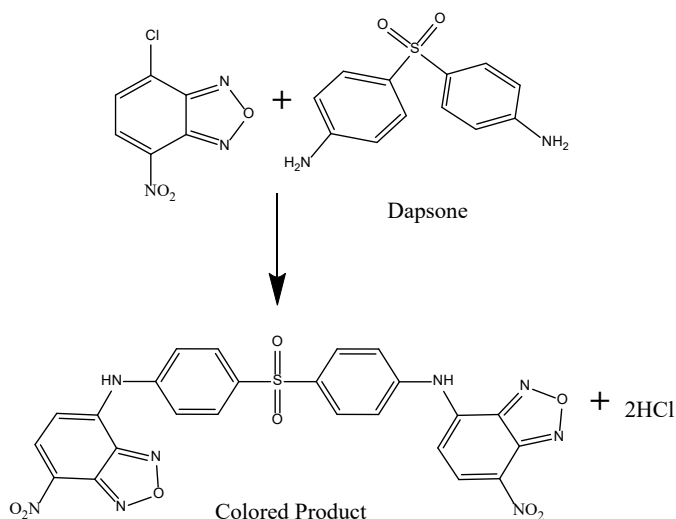


Fig. 5. The reaction equations between Dapsone and NBD-Cl.

the materials, while those with an internal diameter of 0.05 cm are used as reaction coils. This proposed method was based on the targeted drug's combination with NBD-Cl in an alkaline solution to produce a colored compound with a maximum absorbance $\lambda_{\max} = 468$ nm. The amino group on the dapsone structure combines with NBD-Cl to create a colorful complex. [19 - 22]. The chemical equations combining dapsone and NBD-Cl are shown in Fig. 4. In comparison to dapsone (300 nm), the product's wavelength was shifted 168 nm to the long wave. Also, dapsone may be detected in the visible light spectrum. Due to significant potential interference, the detection of dapsone in bimolecular analysis may be prevented. The main benefit of this approach is that dapsone wavelength was moved from the range of ultraviolet light to the range of visible light, allowing for its detection in this range. The technique is easy to apply and can be used to determine how much dapsone is in the tablets.

RESULTS AND DISCUSSION

Absorption spectra

The solution of dapsone is colorless. It does not contain any absorbance in the spectral region of 340 - 468 nm, and its $\lambda_{\max} = 300$ nm. The NBD-Cl-dapsone complex may be easily identified at 468 nm against a solution blank, even though the maximum absorbance wavelength of NBD-Cl is 340 nm. Fig. 6 shows that the colored complex solution has a peak at 468 nm. Between the absorbance and the dapsone concentration, there was an outstanding linear relationship ($R = 0.999$).

Analysis of optimal conditions

Ligand (NBD-Cl) concentration effect

The impact of the NBD-Cl amount was investigated with range values between 0.01 % and 0.04 % after selecting the optimal shape of the TAS manifold (Fig. 5),

under the conditions tested. 0.03 % of NBD-Cl was the amount at which the optimum result occurred, as shown by the outcomes in Table 1 and Fig. 7.

NaOH Concentration effect

The influence of NaOH concentration was also examined. after standardizing the NaOH, (by titrating it against an accurately weighed sample of potassium acid phthalate KHP), utilized to dissolve Dapsone, the range of concentrations that produced the best results was 0.01 mol L⁻¹, according to Table 2 and Fig. 8.

Flow rate effect

At the flow rate range of 70 - 110 $\mu\text{L min}^{-1}$, the impact of the flow rate on the peak height was investigated (Table

3, Fig. 9). Reduced flow rates result in double peaks, presumably as a result of insufficient carrier solution dispersion into the sample zone's middle 18. On the reverse side, as the flow rate increased, the peak height dropped [19]. For the following test, the flow rate was chosen at 100 $\mu\text{L min}^{-1}$ due to its greatest sensitivity, considering the stability of the pump, the peak form, and the sampling period [21 - 24].

Reaction coil length effect

Several reaction coil lengths (30 - 125 cm) were used in this work, with a flow rate of 100 $\mu\text{L min}^{-1}$ and Dapsone quantities of 100 $\mu\text{g mL}^{-1}$. It was found that the selectivity of the response increased at a coil length of 60 cm [23 - 26]. The findings in Table 4 and Fig. 10.

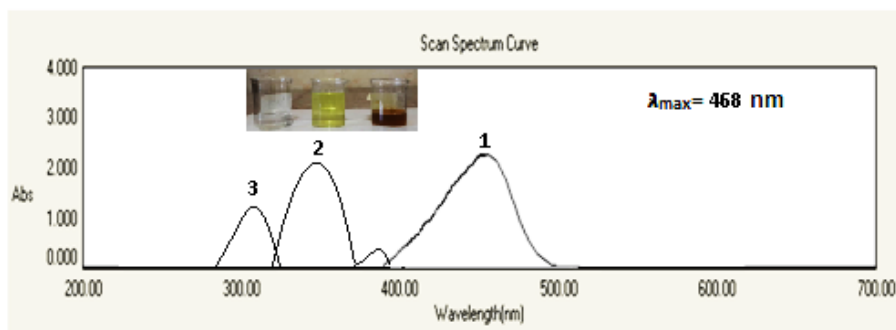


Fig.6. The UV-Vis spectrum of the product (Dapsone- NBD-Cl).

Table 1. The impact of the NBD-Cl amount on the peak height.

[NBD-Cl], %	Height of peaks, cm			Mean \bar{Y}	SD	RSD, %
0.01	3.30	3.30	3.30	3.3000	0.0000	0.0000
0.02	4.50	4.50	4.50	4.5000	0.0000	0.0000
0.03	5.30	5.25	5.25	5.2667	0.0288	0.5481
0.04	4.70	4.70	4.80	4.7333	0.0577	1.2197

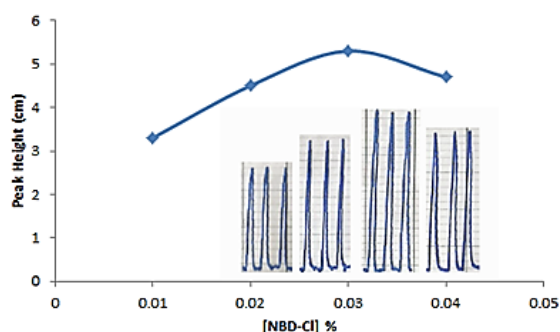


Fig. 7. Impact of the NBD-Cl amounts on the peak height.

Table 2. Impact of the NaOH amounts on the peak height.

NaOH, mol L ⁻¹	Height of peaks, cm			Mean \bar{Y}	SD	RSD, %
0.005	3.50	3.50	3.50	3.500	0.000	0.000
0.010	5.25	5.25	5.25	5.250	0.000	0.000
0.015	4.80	4.80	4.80	4.800	0.000	0.000
0.020	4.50	4.50	4.50	4.500	0.000	0.000

Table 3. The peak height's relationship with flow rate.

Flow rate, $\mu\text{L min}^{-1}$	Height of peaks, cm			Mean \bar{Y}	SD	RSD, %
70.00	4.80	4.80	4.80	4.8000	0.0000	0.0000
80.00	5.30	5.25	5.25	5.2667	0.02887	0.5481
90.00	5.50	5.40	5.50	5.4667	0.0577	1.0561
100.00	5.80	5.80	5.80	5.8000	0.0000	0.0000
110.00	5.60	5.60	5.60	5.6000	0.0000	0.0000

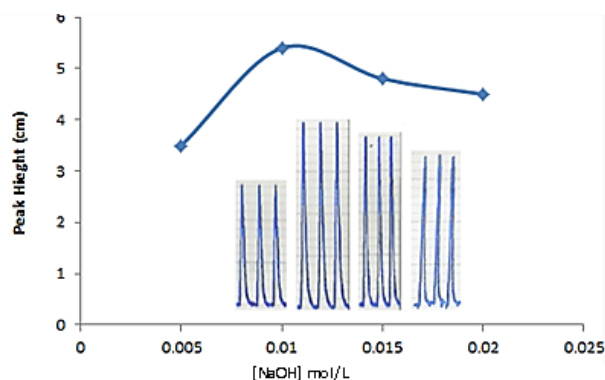


Fig. 8. Effect of NaOH concentration on the response.

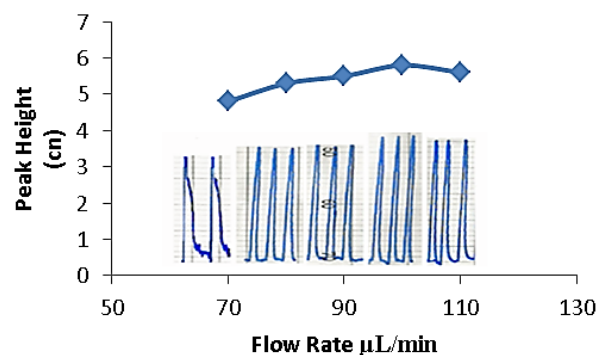
Fig. 9. The response as a function of flow rate ($\mu\text{L min}^{-1}$).

Table 4. The association between the response and reaction coil lengths.

Length of reaction coil, cm	Height of peaks, cm			Mean \bar{Y}	SD	RSD, %
30	4.30	4.30	4.30	4.3000	0.0000	0.0000
60	6.00	6.00	6.00	6.0000	0.0000	0.0000
100	5.60	5.60	5.60	5.6000	0.0000	0.0000
125	5.30	5.25	5.25	5.2667	0.0288	0.5481

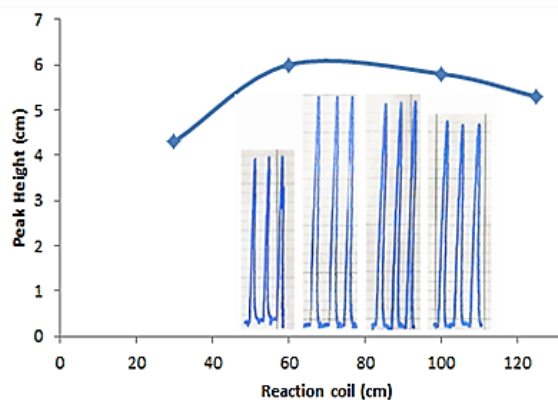


Fig. 10. The impact of reaction coil lengths on response selectivity.

Dapsone volume effect

Several volumes (3.2 - 6.4 μL) of injection were used to test the effect of sample volume on peaks. After 4 μL , the peak height declined. The peak height grew to its maximum at 4 L. Hence, the 4 μL was selected for additional investigation (Table 5, Fig. 11).

The NBD-Cl volume effect

The injection of various volumes (3.2 - 6.4 μL) was done to study the impact of the NBD-Cl volume on the peaks. After 4.8 μL , the peak height decreased. The peak height reached its maximum at that volume. As a result, Table 6 and Fig. 12 selected the 4.8 μL for further research.

The determination of dead volume

We should be examined to guarantee accurate results from this section. Where there is little dead volume, the outcomes are best. There was no response in either of

the two tests that were performed; in the first, water was used as the reagent rather than Dapsone in the loop, and in the second, water was used as the carrier rather than NBD-Cl. This demonstrates the system's effectiveness, as shown in Fig. 13.

Reproducibility

By utilizing repeatability injections of 30 ppm and 60 ppm of dapsone, the prediction range and efficient method of determining dapsone were explored. Table 7 and Fig. 14 display the findings.

Establishing dispersion

One of the significant physical phenomena is dispersion. The coefficient of dispersion is the most widely used exploratory measure to determine the level of dilution of the sample from the inlet to its passage before the spectrometer. Its definition is the percentage

Table 5. The connection between the responses and the volume of Dapsone.

Loop of DAP, cm	Dapsone volume, μL	Height of peaks, cm			Mean \bar{Y}	SD	RSD, %
40	3.2	4.40	4.30	4.30	4.3333	0.0577	1.3323
50	4.0	6.00	6.00	6.00	6.0000	0.0000	0.0000
60	4.8	5.80	5.80	5.80	5.8000	0.0000	0.0000
70	5.6	5.50	5.48	5.48	5.4867	0.0115	0.2104
80	6.4	4.40	4.50	4.50	4.4667	0.0577	1.2926

Table 6. The impact of NBD-Cl volume on wave height.

Loop of NBD-Cl, cm	NBD-Cl volume, μL	Height of peaks, cm			Mean \bar{Y}	SD	RSD, %
40	3.2	4.20	4.20	4.20	4.2000	0.0000	0.0000
50	4.0	6.10	6.10	6.00	6.0667	0.0577	0.9516
60	4.8	6.90	6.90	6.90	6.9000	0.0000	0.0000
70	5.6	6.30	6.30	6.10	6.2333	0.1154	1.8524
80	6.4	6.00	6.00	6.00	6.0000	0.0000	0.0000

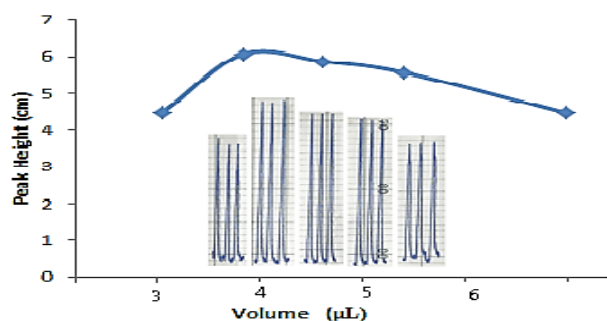


Fig. 11. The responses as a function of Dapsone volume.

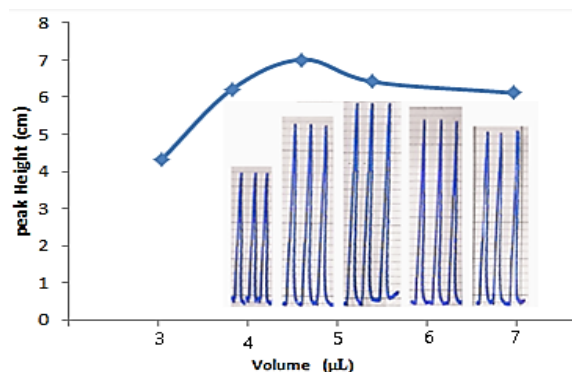


Fig.12. Changing the peak height with NBD-Cl volume.

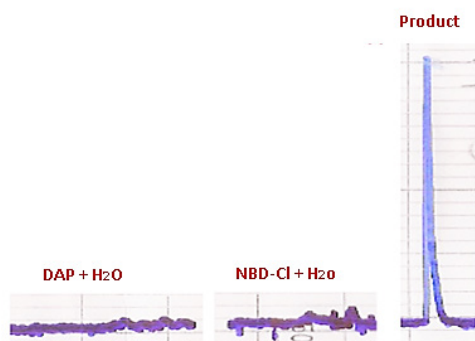


Fig. 13. The study of dead volume.

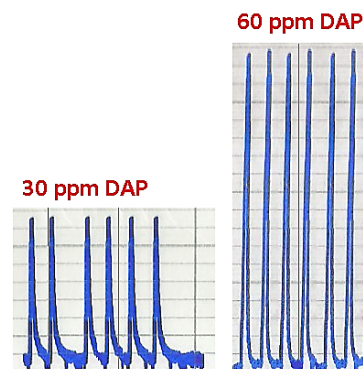


Fig. 14. The repeatability of responses.

Table 7. The repeatability of responses.

Dapsone amounts, mg L ⁻¹	Height of peaks, cm						Mean \bar{Y}	SD	RSD, %
30	2.00	2.00	2.00	2.00	2.00	2.00	2.0000	0.0000	0.0000
60	4.19	4.20	4.19	4.20	4.19	4.20	4.1950	0.0055	0.1306

Table 8. Calculation of dispersion.

Dapsone amounts, $\mu\text{g mL}^{-1}$	Response, cm		Dispersion, D
	H _{max}	H _o	
60	4.20	4.50	1.07
90	6.25	6.75	1.08

of the concentration that occurred prior to and following the dispersion procedure in those components of liquid. It is stated in Eq. 1 [27]:

$$D = \frac{H_o}{H_{max}} \quad (1)$$

where: H_o - peak height without dilution outside the μTAS ; H_{max} - peak height with dilution inside the μTAS system.

Dispersion was 1.07 and 1.08, respectively, for the two concentrations of Dapsone, 60 and 90 $\mu\text{g mL}^{-1}$. These numbers reflect the manifold's limit dispersion. In light of the findings in Table 8 and Fig. 15.

Standard Calibration Curve for Dapsone

The calibration graph was created under ideal conditions and with several amounts of dapsone, the results are shown in Table 9 and Fig. 16. In the concentration range of 0.5 to 100 $\mu\text{g mL}^{-1}$, the calibration curve is linear [28, 29]. The limit of detection which was calculated based on the standard deviation of the

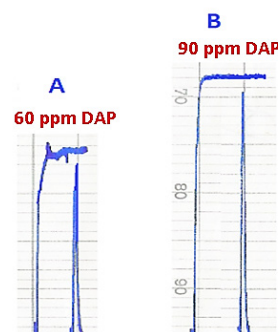


Fig. 15. The dispersion at the different doses of 60 and 90 $\mu\text{g L}^{-1}$

response (Sy) of the curve and the slope of the calibration curve (S) at levels approximating the LOD according to the formula: $\text{LOD} = 3.3(\text{Sy}/\text{S})$, is good and stable at 0.399 $\mu\text{g mL}^{-1}$. Table 10. An overview of the statistical analyses [30 - 32].

The application μTAS method for Determination of dapsone in medicines.

The evaluation of dapsone in tablet form and the generated solution was satisfactorily completed using the suggested methodology. The outcomes achieved demonstrate excellent agreement with the product's labeled information as well as between the taken dose and the recovered quantities of dapsone, as indicated in Table 11.

Table 9. The calculations related to Calibration graph of this method.

Dapsone amounts, $\mu\text{g mL}^{-1}$	Height of peaks, cm			Mean \bar{Y}	SD	RSD, %	$\bar{Y} \pm t_{(0.05/2), n-1} \frac{S.D}{\sqrt{n}}$
0.5	0.35	0.35	0.35	0.3500	0.0000	0.0000	0.3500
1.0	0.60	0.60	0.60	0.6000	0.0000	0.0000	0.6000
5	1.60	1.60	1.65	1.6233	0.0288	1.7856	1.6233 ± 0.0458
10	2.10	2.10	2.00	2.0667	0.0577	2.6646	2.0667 ± 0.0918
20	2.40	2.40	2.40	2.4000	0.0000	0.0000	2.4000
30	3.50	3.50	3.50	3.5000	0.0000	0.0000	3.5000
40	4.18	4.20	4.20	4.1933	0.1154	0.2753	4.1933 ± 0.0918
60	4.90	4.90	4.90	4.9000	0.0000	0.0000	4.9000
80	5.40	5.40	5.40	5.4000	0.0000	0.0000	5.4000
90	6.30	6.30	6.30	6.3000	0.0000	0.0000	6.3000
100	7.00	7.00	7.00	7.0000	0.0000	0.0000	7.0000

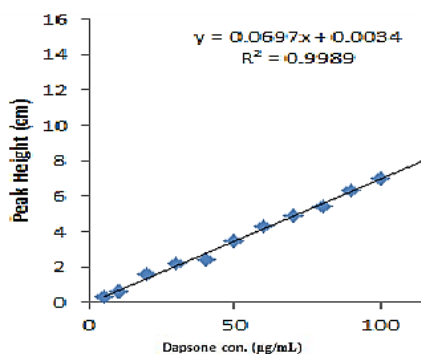


Fig. 16. The calibration graph for variable Dapsone concentrations.

Table 10. The statistical treatments for the calibration graphs by using μ TAS.

Parameters	Value
λ_{max}	468 nm
Flow rate	$100 \mu\text{L min}^{-1}$
Reaction coil length	60.00 cm
DAP volume	$4 \mu\text{L}$
NBD-Cl volume	$4.8 \mu\text{L}$
Cons. of NaOH	0.01 M
Cons. of NBD-Cl	0.03 %
Linearity range	$0.5 - 100 \mu\text{g mL}^{-1}$
Regression equation	$Y = 0.0697X + 0.0034$
Regression coefficient (R^2)	0.9989
Correlation coefficient (R)	0.9994
Standard deviation of the residuals, $Sy/x = [\sum (y_i - \bar{y}_i)^2 / (n - 2)]^{0.5}$; $\bar{y}_i = b x_i + a$	0.0284
Standard deviation of the slope, $S_b = Sy/x / [\sum (x_i - \bar{x})^2]^{0.5}$	1.4025×10^{-4}
RSD % for (6) determination of standards $60 \mu\text{g mL}^{-1}$	0

Table 11. Application of the suggested method (μ TAS) to determine of dapsons.

Pharmaceutical preparation	Present, $\mu\text{g mL}^{-1}$	Found, $\mu\text{g mL}^{-1}$	E_{error} , %	Rec, %	RSD, %
Dapsone in tablet	10.00	10.05	0.2400	100.24	0.11
	20.00	20.09	0.3000	100.30	0.32

CONCLUSIONS

The suggested system μ TAS is a novel procedure to determine dapsons. The μ TAS is not required to use microchips. This strategy produces outcomes that are simple, quick, cheap, and accurate. The main benefit of the suggested method is that it can be used to measure the amount of dapsons in tablets at a low cost.

REFERENCES

- J. Watanabe, J. Shimamoto, K. Kotani, The effects of antibiotics for helicobacter pylori eradication or dapsons on chronic spontaneous urticaria: A systematic review and meta-analysis, *Antibiotics*, 10, 2021, 156.
- R. Tiwari, G. Tiwari, P. Wal, A. Wal, P. Maurya, Development, characterization and transdermal delivery of dapsons and an antibiotic entrapped in ethanoic liposomal gel for the treatment of lepomatous leprosy, *The Open Nanomedicine J.*, 5, 2018,1-15.
- P.D. Tzanavaras, E. Thiakouli, D.G. Themelis, Hybrid sequential injection-flow injection manifold for the spectrophotometric determination of total sulfite in wines using o-phthalaldehyde and gas-diffusion, *Talanta*, 77, 2009, 1614-1619. <https://doi.org/10.1016/j.talanta.2008.09.051>
- J. Ghusoon, N. Dakhil, S. Muthana, New flow injection designed unit for the determination of dapsons in some pharmaceutical products, *Inter. J. Chem.Tech. Res.*, 9,11, 2019, 391-400.
- D.T. Emmanouil, A. L. Joao, H.Eddo, E.Hendrik, Development and validation of a multi-analyte GC-MS method for the determination of 84 substances from plastic food contact materials, *Anal. Bioanal. Chem.*, 412, 2020, 5419-5434.
- V. Santosh, S. Madhuri, Development and validation of stability indicating HPLC method for estimation of Dapsone, *Int. J. Pharma. Res. Health Sci.*, 2018, 6, 2, 2517-2521.
- S.V. Gandhi, G.R. Patil, Development and validation of stability-indicating HPTLC method for estimation of Dapsone, *European J. Biomedical and Pharmaceutical Sciences*, 6,1, 2018, 322-329.
- M. Bahaa, S. Amer, J. Thulfiqar, E. Keith, Mutual derivatization in the determination of Dapsone and Thymol using cloud point extraction followed by spectrophotometric detection, *Anal. Bioanal. Chem. Res.*, 8, 2, 177-186, 2021.
- M.S. Al-Enizzi1, O.A.S. Ahmad, T.N. Al-Sabha, Spectrophotometric determination of Dapsone using charge transfer complex formation reaction, *Egypt. J. Chem.*, 63, 8, 2020, 3167-3177.
- M.T. Al-Obaidi, T.N. Al-Sabha, T.S. Al-Ghabsha, Spectrophotometric determination of Nitrazepam and Dapsone using vanillin reagent in pharmaceutical preparations, *J. Edu. Sci.*, 2014, 27, 1, 43-57.
- P. Nagaraja, A.K. Shrestha, A.S. Kumar, A.K.Gouda, Use of N,N-diethyl-phenylenediaminesulphate for the spectrophotometric determination of some phenolic and amino drugs, *Acta Pharma*, 60, 2010, 217-227.
- S.S.M.P. Vidigal, A.O.S.S. Rangel, Exploiting flow-based separation techniques for sample handling in wine analysis, *Food Anal. Methods*, 15, 2022, 565-578. <https://doi.org/10.1007/s12161-021-02138-6>
- S.S.M.P. Vidigal, A.O.S.S. Rangel, A flow-based platform for measuring the acidity parameters in wine, *Talanta*, 168, 2017, 313-319. <https://doi.org/10.1016/j.talanta.2017.03.029>
- E.W. Damith, J. Shu, S. Jay, S. Jalal, S. Kathleen, T.C. Christopher, Micro total analysis systems: Fundamental advances and applications, *Article in Analytical Chem.*, 2015.
- N. Olgun, S. Erturk, S. Atmaca, Spectrofluorometric and spectrophotometric methods for the determination of vigabatrin in tablets, *J. Pharmaceut.*

- Biomed. Anal., 29, 2002, 1-5.
16. A.T. Elham, Kinetic spectrophotometric methods for the determination of dothiepin hydrochloride in bulk and in drug formulation, *Anal. Bioanal. Chem.*, 376, 2003, 1131-1136.
17. I.A. Darwish, Kinetic spectrophotometric methods for determination of trimetazidinedihydrochloride, *Anal. Chem. Acta*, 551, 2005, 222-231.
18. E.A. Azooz, G.J. Shabaa, E.H.B. Al-Muhanna, E.A.J. Al-Mulla, W.I. Mortada, Displacement cloud point extraction procedure for preconcentration of iron (III) in water and fruit samples prior to spectrophotometric determination, *Bull. Chem. Soc. Ethiop.*, 37, 1, 2023, 1-10. <https://dx.doi.org/10.4314/bcse.v37i1.1>
19. V. Cerdà, L. Ferrer, J. Avivar, A. Cerdà, Chapter 1 - Evolution and Description of the Principal Flow Techniques, *Flow Analysis. A Practical Guide*, 2014, 1-42.
20. E.A. Azooz, G.J. Shabaa, E.A.J. Al-Mulla, methodology for preconcentration and determination of silver in aqueous samples using cloud point extraction, *Braz. J. Anal. Chem.* 9,35, 2022, 39-48. doi: <http://dx.doi.org/10.30744/brjac.2179-3425>. AR-61-2021
21. D.E.W. Patabadige, S. Jia, J. Sibbitts, J. Sadeghi, K. Sellens, C.T. Culbertson, Micro total analysis systems: Fundamental advances and applications, *Anal. Chem.*, 2016, 88, 1, 320-338. <https://doi.org/10.1021/acs.analchem.5b04310>
22. I.A. Mohammed, E.A.J. Al-Mulla, N.K.A. Kadar, Structure-property studies of thermoplastic and thermosetting polyurethanes using palm and soya oils-based polyols, *J. Oleo Sci.*, 2013, 62, 12, 1059-1072. <https://doi.org/10.5650/jos.62.1059>
23. E.A.J. Al-Mulla, Preparation of polylactic acid/epoxidized palm oil/fatty nitrogen compounds modified clay nanocomposites by melt blending, *Polym. Sci., Series A*, 53, 2, 2011, 149-157.
24. F.H.J. Al-Shemmari, E.A.J. Al-Mulla, A.A. Rbah, A comparative study of different surfactants for natural rubber clay nanocomposite preparation, *Rendiconti Lincei*, 25, 3, 2014, 409-413. <https://doi.org/10.1007/s12210-014-0307-z>
25. G.J. Shabaa, F.A. Semysim, R.K. Ridha, E.A. Azooz, E.A.J. Al-Mulla, Air-assisted dual-cloud point extraction coupled with flame atomic absorption spectroscopy for the separation and quantification of zinc in pregnant women's serum. *J. Iran. Chem. Soc.*, 20, 2023, 2277-2284, <https://doi.org/10.1007/s13738-023-02834-6>
26. W.H. Hoidy, M.B. Ahmad, E.A.J. Al-Mulla, Chemical synthesis and characterization of palm oil-based difatty acyl thiourea, *J. Oleo Sci.*, 2010, 59,5, 229 - 233. <https://doi.org/10.5650/jos.59.229>
27. L.C. Duarte, I. Pereira, L.I.L. Maciel, B.G. Vaz, W.K.T. Coltro, 3D printed microfluidic mixer for real-time monitoring of organic reactions by direct infusion mass spectrometry, *Analytica Chimica Acta*, 2022, 1190, 339252. <https://doi.org/10.1016/j.aca.2021.339252>
28. J.N. Miller, J.C. Miller, *Statistics and Chemical Metrics for Analytical Chemistry*, 6th edition, Pearson Education Limited, UK, 2010.
29. J. Sibbitts, K.A. Sellens, S. Jia, S.A. Klasner, C.T. Culbertson, Cellular analysis using microfluidics, *Anal. Chem.*, 90, 1, 2018, 65-85. <https://doi.org/10.1021/acs.analchem.7b04519>
30. E.A. Azooz, F.A. Wannas, S.K. Jawad, Developed cloud point extraction coupled with onium system for separation and determination cobalt in biological samples, *Research Journal of Pharmacy and Technology*, 2021, 14, 2, 594-598.
31. Y. Liu, L. Sun, H. Zhang, L. Shang, Y. Zhao, Microfluidics for drug development: from synthesis to evaluation, *Chemical Reviews*, 2021, 121,13, 7468-7529. <https://doi.org/10.1021/acs.chemrev.0c01289>
32. A.R. Hussein, M.S. Gburi, N.M. Muslim, E.A. Azooz, A greenness evaluation and environmental aspects of solidified floating organic drop microextraction for metals: A review, *Trends Environ. Anal. Chem.*, 37, 2023, e00194. <https://doi.org/10.1016/j.teac.2022.e00194>